



Two Small Transiting Planets and a Possible Third Body Orbiting HD 106315

Ian J. M. Crossfield^{1,12}, David R. Ciardi², Howard Isaacson³, Andrew W. Howard⁴, Erik A. Petigura^{5,13}, Lauren M. Weiss^{6,14}, Benjamin J. Fulton^{4,7,15}, Evan Sinukoff^{4,7,16}, Joshua E. Schlieder^{2,8}, Dimitri Mawet⁴, Garreth Ruane⁴, Imke de Pater³, Katherine de Kleer³, Ashley G. Davies⁹, Jessie L. Christiansen², Courtney D. Dressing^{5,12}, Lea Hirsch³, Björn Benneke⁵, Justin R. Crepp¹⁰, Molly Kosiarek¹, John Livingston¹¹, Erica Gonzales^{1,10}, Charles A. Beichman², and Heather A. Knutson⁵

¹Astronomy and Astrophysics Department, UC Santa Cruz, CA, USA

²NASA Exoplanet Science Institute, California Institute of Technology, Pasadena, CA, USA

³Astronomy Department, University of California, Berkeley, CA, USA

⁴Astronomy Department, California Institute of Technology, Pasadena, CA, USA

⁵Geological and Planetary Sciences, California Institute of Technology, Pasadena, CA, USA

⁶Institute for Research on Exoplanets, University of Montreal, Canada

⁷Institute for Astronomy, University of Hawai'i at Mānoa, Honolulu, HI, USA

⁸NASA Goddard Space Flight Center, Greenbelt, MD, USA

⁹NASA Jet Propulsion Laboratory, Pasadena, CA, USA

¹⁰Department of Physics, University of Notre Dame, 225 Nieuwland Science Hall, Notre Dame, IN, USA

¹¹Department of Astronomy, The University of Tokyo, 7-3-1 Bunkyo-ku, Tokyo 113-0033, Japan

Received 2017 January 13; revised 2017 February 13; accepted 2017 February 15; published 2017 May 19

Abstract

The masses, atmospheric makeups, spin–orbit alignments, and system architectures of extrasolar planets can be best studied when the planets orbit bright stars. We report the discovery of three bodies orbiting HD 106315, a bright ($V = 8.97$ mag) F5 dwarf targeted by our *K2* survey for transiting exoplanets. Two small transiting planets are found to have radii $2.23^{+0.30}_{-0.25} R_{\oplus}$ and $3.95^{+0.42}_{-0.39} R_{\oplus}$ and orbital periods 9.55 days and 21.06 days, respectively. A radial velocity (RV) trend of $0.3 \pm 0.1 \text{ m s}^{-1} \text{ day}^{-1}$ indicates the likely presence of a third body orbiting HD 106315 with period $\gtrsim 160$ days and mass $\gtrsim 45 M_{\oplus}$. Transits of this object would have depths $\gtrsim 0.1\%$ and are definitively ruled out. Although the star has $v \sin i = 13.2 \text{ km s}^{-1}$, it exhibits a short-timescale RV variability of just 6.4 m s^{-1} . Thus, it is a good target for RV measurements of the mass and density of the inner two planets and the outer object's orbit and mass. Furthermore, the combination of RV noise and moderate $v \sin i$ makes HD 106315 a valuable laboratory for studying the spin–orbit alignment of small planets through the Rossiter–McLaughlin effect. Space-based atmospheric characterization of the two transiting planets via transit and eclipse spectroscopy should also be feasible. This discovery demonstrates again the power of *K2* to find compelling exoplanets worthy of future study.

Key words: eclipses – stars: individual (HD 106315) – techniques: photometric – techniques: spectroscopic

1. Introduction

Planets smaller than Neptune ($R_p \lesssim 4 R_{\oplus}$) are the most common type of planet, both in terms of total detections (Coughlin et al. 2016) and intrinsic occurrence (Howard et al. 2010b, 2012; Dressing & Charbonneau 2013, 2015; Fressin et al. 2013; Petigura et al. 2013b). Most of these small planets were discovered by NASA's *Kepler Space Telescope* during its prime mission (2009–2013; Borucki et al. 2010). However, *Kepler* surveyed only 1/400th of the sky and thus typically detected planets orbiting relatively faint stars: extremely useful for demographic studies, but less so for detailed characterization of planet masses, spin–orbit alignments, and atmospheric properties. Small planets orbiting bright host stars are essential to enable the

precise measurements best-suited to reveal the formation, composition, structure, and evolution of these systems.

For planets of a fixed size between 2 and $4 R_{\oplus}$, the observed masses span an order of magnitude (Marcy et al. 2014; Berta-Thompson et al. 2015; Wolfgang et al. 2016). This result indicates that for a given planet size, many possible bulk compositions are possible. Radial velocity (RV) measurements can determine the mass of a transiting planet and so constrain its fractional makeup of metal, rock, ice, and gas (H_2/He). Mass and radius measurements alone do not uniquely determine the bulk makeup of sub-Jovians with radii $\gtrsim 1.5 R_{\oplus}$ (Figueira et al. 2009; Rogers & Seager 2010; Rogers et al. 2011); further detailed inferences are more difficult when considering that the atmospheres of these smaller planets may be enhanced in metals by factors of tens to thousands depending on how the planets formed and migrated (Fortney et al. 2013; Moses et al. 2013). Atmospheric measurements are needed to assess the elemental composition of these planets' atmospheres (Crossfield 2015), while measurements of the Rossiter–McLaughlin (RM) effect can constrain planet migration histories and stellar interiors (Winn & Fabrycky 2015). Furthermore, there is growing interest in comparing all of these quantities of planets orbiting single stars with those of planets orbiting multi-star (or star-brown dwarf) systems.

¹² NASA Sagan Fellow.

¹³ Hubble Fellow.

¹⁴ Trotter Fellow.

¹⁵ NSF Graduate Research Fellow.

¹⁶ NSERC Postgraduate Research Fellow.



As a transit survey, *K2* lies in the sweet spot between *Kepler* and *TESS* in terms of sky coverage, temporal duration, photometric precision, and the discovery rate of new candidates (Howell et al. 2014; Ricker et al. 2014; Sullivan et al. 2015). Hundreds of planets have been discovered from the *K2* mission, increasing the number of bright systems ($J = 8 - 12$ mag) known to host small planets ($1-4 R_{\oplus}$) by over 50% in just its first year (Crossfield et al. 2016; Vanderburg et al. 2016c). Systems such as K2-3, HD 3167, and HIP 41378 are some of the most interesting of *K2*'s multi-planet discoveries, mainly because they are especially good targets for RV and atmospheric measurements (Crossfield et al. 2015; Vanderburg et al. 2016a, 2016b).

Here, we present the discovery of another new multi-planet system around a bright star observed by *K2*: two small planets transiting the F dwarf HD 106315 (EPIC 201437844) and a likely RV trend that would indicate a third body on a long-period orbit. The system promises to be a good target for future RV measurements to explore the system architecture and planet mass and spin-orbit alignment, and for future atmospheric characterization. We describe our discovery, observations, and derived system properties in Section 2 and summarize and discuss the potential for future observations in Section 3.

2. Observations and Analysis

HD 106315 was proposed as a *K2* target for Campaign 10 (C10) in three programs: GO-10028 (PI Quarles), GO-10051 (PI Cochran), and by our team's GO-10077 (PI Howard). The star's basic parameters are listed in Table 1. It and other targets in C10 were scheduled to be observed for the usual ~ 75 -day duration, but during C10's first six days, the spacecraft mispointed by 3.3 pixels ($13''$). Data acquired during these first six days is therefore of low quality and so we discard these early data. Of the remaining time in C10, a fault with one of the spacecraft's photometry modules caused an additional 14 days to be lost before the final 7 weeks of C10 observations (see Figure 1).

2.1. *K2* Photometry

We convert the processed *K2* target pixel files from C10 into light curves and search for transits using the same approach as described in our previous papers (e.g., Crossfield et al. 2016; Sinukoff et al. 2016). Our light curves at each step in our analysis are shown in Figure 1. In brief, we use the publicly available *k2phot* photometry code¹⁷, which uses Gaussian Processes to model out systematics associated with the ~ 1 pixel pointing jitter of the spacecraft that occurs over ~ 6 hr timescales. We then use the publicly available TERRA algorithm¹⁸ (Petigura et al. 2013a, 2013b) to search for transit-like events and manually examine light curves and diagnostic plots for all plausibly transit-like signals for signal-to-noise ratio (S/N) ≥ 12 . We discovered a signal with period $P = 9.55$ days in the photometry for HD 106315. Inspection of the light curve revealed two deeper transits separated by 21 days; a third event was presumably missed during C10's 14 day data gap (see Figure 1).

As in our previous work, light-curve fits and an MCMC analysis provide orbital and system parameters (emcee and

Table 1
Stellar Parameters of HD 106315

Parameter	Value	Source
<i>Identifying information</i>		
α R.A. (hh:mm:ss)	12:13:53.39	...
δ decl. (dd:mm:ss)	-00:23:36.54	...
EPIC ID	201437844	Huber et al. (2016)
<i>Photometric Properties</i>		
B (mag)	9.402 ± 0.022	APASS
V (mag)	8.951 ± 0.018	APASS
g (mag)	10.14 ± 0.19	APASS
r (mag)	9.41 ± 0.29	APASS
i (mag)	8.848 ± 0.060	APASS
J (mag)	8.116 ± 0.025	2MASS
H (mag)	7.962 ± 0.040	2MASS
K_s (mag)	7.853 ± 0.020	2MASS
W1 (mag)	7.794 ± 0.025	AllWISE
W2 (mag)	7.850 ± 0.020	AllWISE
W3 (mag)	7.839 ± 0.022	AllWISE
W4 (mag)	8.168 ± 0.354	AllWISE
<i>Spectroscopic and Derived Properties</i>		
μ_{α} (mas yr ⁻¹)	-1.68 ± 0.64	GAIA (2016)
μ_{δ} (mas yr ⁻¹)	11.91 ± 0.46	GAIA (2016)
Distance (pc)	107.3 ± 3.9	GAIA (2016)
Age (Gyr)	4 ± 1 Gyr	HIRES, this paper
Spectral Type	F5V	Houk & Swift (1999)
[Fe/H]	-0.24 ± 0.04	HIRES; SM
T_{eff} (K)	6290 ± 60	HIRES; SM
$\log_{10} g$ (cgs)	4.29 ± 0.07	HIRES; SM
$v \sin i$ (km s ⁻¹)	13.2 ± 1.0	HIRES; SM
S_{HK}	0.1400 ± 0.0005	HIRES
M_* (M_{\odot})	1.07 ± 0.03	HIRES; SM; iso
R_* (R_{\odot})	1.18 ± 0.11	HIRES; SM; iso
L_* (L_{\odot})	1.95 ± 0.38	HIRES; SM; iso
dv/dt (m s ⁻¹ day ⁻¹)	0.3 ± 0.1 m s ⁻¹ day ⁻¹	HIRES

Note. SM: SpecMatch (Petigura 2015). iso: isochrones (Morton 2012).

BATMAN; Foreman-Mackey et al. 2012; Kreidberg 2015) whose final distributions are unimodal. We impose priors on the stellar limb profile using a quadratic parametrization, with values and uncertainties derived from PyLDTK (Parviainen & Aigrain 2015). Our previous analyses show that this choice does not strongly affect the system parameters we measure (Crossfield et al. 2016). Figure 1 shows the resulting photometry and best-fit models, and Table 2 summarizes the final values and uncertainties.

Several other features are also visible in the intermediate panels of Figure 1. First, our data lacks coverage during the transit egress of HD 106315 b, because several *K2* thruster-firings occur during this time. We did examine *K2*'s early (mispointed) observations of this system, in which we see another transit of HD 106315 b, with consistent depth (albeit at low S/N). We also see planet b's transits in the photometry provided by the *Kepler* Project Office, though these data are of lower quality than ours. We see a few low points that occur together near time index 2750; we attribute these to uncorrected systematics rather than a transiting object, because we do not see additional transits at this depth and because these data occur at the beginning of *K2*'s observations (when we see a strong ramp in the decorrelated data).

We also see several transit-like events in the decorrelated flux panel of Figure 1, the most convincing of which occurs at time index 2790. We fit a transit model to these data and run an

¹⁷ <https://github.com/petigura/k2phot>

¹⁸ <https://github.com/petigura/terra>

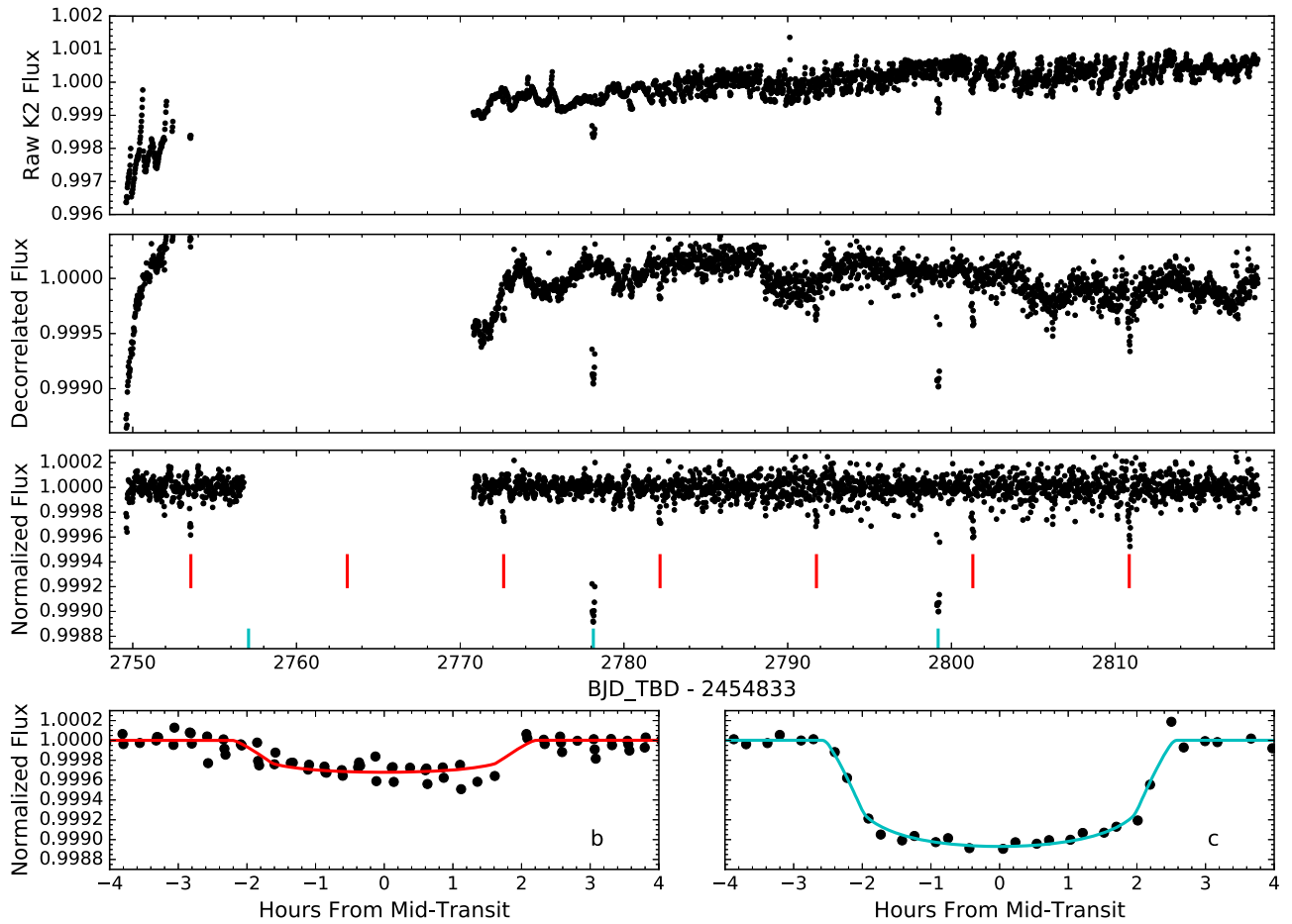


Figure 1. From top to bottom: our *K2* photometry extracted from *K2* pixel-level data; the data after decorrelation with *k2phot*; the data after smoothing and detrending, with vertical ticks indicating the locations of each planet’s transits; and, at bottom, the phase-folded photometry and best-fit light curves for each transiting planet.

Table 2
Planet Parameters

Parameter	Units	b	c
T_0	BJD _{TDB} - 2454833	$2772.6521^{+0.0042}_{-0.0045}$	$2778.1310^{+0.0012}_{-0.0012}$
P	day	$9.5521^{+0.0019}_{-0.0018}$	$21.0576^{+0.0020}_{-0.0019}$
i	deg	$88.4^{+1.1}_{-2.1}$	$89.42^{+0.40}_{-0.67}$
R_p/R_*	%	$1.708^{+0.188}_{-0.083}$	$3.034^{+0.163}_{-0.067}$
T_{14}	hr	$3.96^{+0.17}_{-0.16}$	$4.693^{+0.078}_{-0.062}$
T_{23}	hr	$3.73^{+0.17}_{-0.19}$	$4.354^{+0.062}_{-0.086}$
R_*/a	...	$0.0599^{+0.0231}_{-0.0065}$	$0.0299^{+0.0056}_{-0.0016}$
b	...	$0.47^{+0.31}_{-0.32}$	$0.34^{+0.28}_{-0.23}$
$\rho_{*,\text{circ}}$	g cm^{-3}	$0.97^{+0.40}_{-0.60}$	$1.60^{+0.28}_{-0.65}$
a	AU	$0.09012^{+0.00083}_{-0.00085}$	$0.1526^{+0.0014}_{-0.0014}$
R_p	R_\oplus	$2.23^{+0.30}_{-0.25}$	$3.95^{+0.42}_{-0.39}$
S_{inc}	S_\oplus	240^{+48}_{-43}	83^{+16}_{-15}

MCMC analysis in which all parameters except e and ω are unconstrained, and we find a mid-time of 2790.382 ± 0.056 and $R/R_* = 0.0133 \pm 0.0012$. However, the event’s profile is asymmetric (with a much shorter ingress than egress), and we see several other features with comparable shapes and amplitudes in our data. Although an intriguing candidate, we cannot conclude that this signal is planetary in origin.

2.2. Ground-based Characterization and Validation

Fortuitously, approximately thirty minutes after identifying HD 106315 as a set of interesting planet candidates, we were able to begin observing the system using both the Keck/HIRES high-resolution optical spectrograph (Vogt et al. 1994) and the Keck adaptive optics (AO) system and NIRC2, its near-infrared camera. Below, we describe the acquisition and analysis of these data.

2.2.1. Keck/HIRES Optical Spectroscopy

We acquired three HIRES exposures of HD 106315 on UT 2016 December 24 to construct a stellar template for RV analysis and for stellar characterization. These observations used the B3 decker, had exposure lengths of roughly 190 s, were acquired in seeing of $1''.0$ – $1''.1$, and did not use the instrument’s iodine gas cell (used for precise RV measurements; see below). We use the SpecMatch algorithm (Petigura 2015) to derive stellar properties from our Keck/HIRES spectrum. The resulting values, shown in Table 1, indicate that HD 106315 is somewhat larger and hotter and rotates more rapidly than the Sun. These stellar parameters are generally consistent with, but more precise than, those derived using broadband photometry and proper motions only (Huber et al. 2016).

We also use the Keck/HIRES spectra to search for evidence of secondary stellar lines, as might be caused by a blended eclipsing binary (Kolbl et al. 2015). We find no evidence of stellar companions down to a sensitivity of 1% of the brightness of the primary. Due to the rapid rotation of HD 106315, we are not sensitive to any star with a relative velocity within 20 km s^{-1} of HD 106315.

The values of $v \sin i$ and R_* derived above indicate a stellar rotation period of ≤ 4.5 days. After masking out transits and the first six days of C10 photometry, a Lomb–Scargle periodogram of the photometry shows a hint of periodicity at $P \approx 5.1$ and ≈ 8.5 days, with amplitudes of 0.1%–0.2%. The former could be marginally consistent with a stellar rotation period if the star is seen nearly equator-on but would be much more rapid than expected from gyrochronology (Ceillier et al. 2016). In either case, the low photometric variability indicates that HD 106315’s surface is relatively unaffected by prominent features such as starspots that would modulate the star’s apparent brightness and induce non-planetary RV signals.

Various sources of error, both instrumental and astrophysical, can mask the Doppler signals from orbiting planets. This RV “noise” is manifest from multiple physical sources that vary with stellar parameters, including temperature, surface gravity, and age (see, e.g., Howard et al. 2010a). For stars cooler than the Sun, rotational modulation of surface features, including faculae and spots, is often the dominant effect (Isaacson & Fischer 2010; Dumusque et al. 2011a, 2011b; Haywood et al. 2014). Granulation and acoustic oscillations are also detectable for magnetically quiet Sun-like stars (Dumusque et al. 2011c). For stars hotter and with lower gravity than the Sun (such as HD 106315), surface oscillations can produce significant false Doppler shifts, and high rotational speeds degrade the quality of the observed spectra, compromising Doppler precision. For A–F type stars, the formula of (Galland et al. 2005) predicts the RV scatter in stars observed at high SNR with Elodie and HARPS, $\sigma_{\text{RV}} \approx 0.16 \times v \sin i^{1.54}$. This formula is accurate at the factor-of-two level and predicts a per-shot RV uncertainty of 8 m s^{-1} for HD 106315, which is comparable to the 6.4 m s^{-1} of scatter that we typically observe on a given night (see below). Surface oscillation amplitudes scale as the light-to-mass ratio, $v_{\text{osc}} = 0.234(L_*/M_*) \text{ m s}^{-1}$ (Kjeldsen & Bedding 1995). Although HD 106315 is hotter than the Sun, $L_*/M_* = 1.8$ and surface oscillations do not dominate.

We obtained several epochs of RV observations of HD 106315 using Keck/HIRES with the standard CPS setup: the C2 decker (for all but the first five RVs, which used the B5 decker), the HIRES iodine cell (used to measure precise RVs; Marcy & Butler 1992), and exposures of 3–6 minutes (depending on seeing conditions). These RV measurements are shown in Table 3.

Although our RV data are not sufficient to robustly measure the masses of our two transiting planets, we examined our measurements in order to better understand the system’s RV behavior. When we subtract each night’s mean from our measurements, the rms of the data drops to 6.4 m s^{-1} , which is our best estimate for the system’s RV noise floor on these timescales. This noise level is sufficiently low that precise RV measurements should eventually be able to constrain the masses of the transiting planets and characterize the third body’s full orbital properties.

We fit several different models to our RV measurements using `radvel`.¹⁹ We examine all cases either including or

Table 3
Keck/HIRES Radial Velocities

HJD (UTC)	RV (m s^{-1})	σ_{RV}^a (m s^{-1})
2457746.13805	5.7	3.9
2457746.14276	−0.3	3.9
2457747.06857	5.9	3.7
2457747.10475	5.5	3.6
2457747.15905	17.2	3.5
2457760.09504	10.7	3.7
2457760.13026	−8.8	3.7
2457760.17270	−2.2	3.8
2457764.01673	12.1	3.8
2457764.05201	8.8	3.6
2457764.08954	5.4	3.5
2457764.09291	11.1	3.6
2457764.09626	15.3	3.6
2457764.13194	−0.6	3.6
2457764.17179	15.4	3.2
2457765.02290	−7.3	3.2
2457765.02811	1.7	3.6
2457765.03199	1.8	3.4
2457765.06751	−3.4	3.4
2457765.14384	1.1	3.1
2457765.15072	−2.7	3.4
2457765.15814	2.1	3.2
2457766.01963	4.6	3.4
2457766.05401	−8.4	3.5
2457766.10269	−14.6	3.4
2457766.13235	−7.8	3.4
2457766.17426	−12.7	3.3
2457775.00259	−12.7	4.4
2457775.08258	−5.6	4.4
2457775.14465	14.0	4.4
2457775.17867	13.1	4.8
2457775.97223	2.9	4.4
2457776.03292	−0.2	4.4
2457776.07229	−2.1	4.3
2457776.11589	−8.8	4.8
2457776.17513	7.8	4.3
2457788.03498	−12.9	4.9
2457788.09157	−15.1	4.8
2457788.14381	4.4	5.0
2457788.96686	−2.1	4.8
2457789.03347	−8.5	4.6
2457789.07500	−19.3	4.9
2457789.12474	−7.6	4.7
2457789.93510	−12.3	4.7
2457789.96977	0.3	5.1
2457790.02547	13.1	4.8
2457790.07589	9.3	5.1
2457790.11559	−0.6	5.5
2457790.94048	0.5	4.2
2457790.98777	6.0	4.2
2457791.02825	2.6	4.2
2457791.06161	2.1	4.1
2457791.13065	−6.2	4.1

Note.

^a An additional 6.4 m s^{-1} was added in quadrature with these uncertainties for the RV analyses described in the text.

omitting a linear trend; a sinusoidal planetary signal phased to planet b’s orbit; a sinusoidal planetary signal phased to planet c; and a two-planet model. In all fits, we hold `radvel`’s “jitter” (extra noise) term fixed at 6.4 m s^{-1} in order to give χ^2

¹⁹ <https://github.com/California-Planet-Search/radvel>

Table 4
Radial Velocity Models

Model	trend ($\text{m s}^{-1} \text{ day}^{-1}$)	K_b (m s^{-1})	K_c (m s^{-1})	dof	χ^2	BIC
2 planets, trend	-0.42 ± 0.10	8.4 ± 2.1	4.8 ± 2.0	50	50.0	370.2
Planet b, trend	-0.287 ± 0.084	6.1 ± 2.0	...	51	56.4	375.6
Planet c, trend	-0.221 ± 0.085	...	1.9 ± 1.7	51	65.1	384.3
No planets, trend	-0.183 ± 0.076	52	66.1	384.4
2 planets, no trend	...	3.5 ± 1.8	0.3 ± 1.6	51	68.2	387.4
Planet b, no trend	...	3.5 ± 1.8	...	52	68.2	386.5
Planet c, no trend	-0.2 ± 1.6	52	71.9	390.1
No planets, no trend	53	71.9	389.1

equal to the number of degrees of freedom for the most complex model considered. Table 4 lists the results of these analyses, including the measured trend and planetary signals (if any) and the χ^2 and Bayesian Information Criterion (BIC).

It is clear from Table 4 that the most favored models all include a linear velocity trend (constant acceleration) with an amplitude of roughly $0.3 \pm 0.1 \text{ m s}^{-1} \text{ day}^{-1}$. The residuals to a trend-only model have an rms of 8.7 m s^{-1} , substantially higher than our night-to-night noise floor reported above; it is therefore likely that additional coherent RV signals are present above the noise floor. Indeed, the most favored model includes a trend and RV signals from both planets, but the planetary semi-amplitudes should be considered preliminary in light of the sparse data coverage, high noise levels, and possibility of additional planetary signals. Nonetheless, the best model without a trend is disfavored by $\Delta\text{BIC} = 16.3$, which strongly indicates the presence of the modeled trend. We also tested models with curvature but find that they do not improve the BIC. Below in Section 3, we discuss the implication of the detected trend.

2.2.2. Keck/NIRC2 AO Imaging

We obtained Keck/NIRC2 AO imaging of HD 106315 on the nights of 2016 December 23, 2017 January 4, and 2017 January 8. Seeing and AO correction were both poor on the first night, but conditions were good on the second night and excellent on the third. We therefore use only the third night’s data. We observed using the Br- γ filter, a narrow-band K-band alternative that allows us to observe HD 106315 without saturating. We used the 1024×1024 NIRC2 array, which has a pixel scale of $9.942 \text{ mas pix}^{-1}$ with the natural guide star system (using HD 106315 as the guide star). A 3-point dither pattern avoided the noisier lower left quadrant of the NIRC2 array. We acquired nine frames with 20 coadds each and a 0.5 s integration time and three frames with 40 coadds of 0.5 s each, for a total of 150 s of on-source exposure time. The data were flat-fielded and sky subtracted and the dither positions were shifted and coadded into a single final image, shown in Figure 2.

The target star was measured with a resolution of 47 mas (FWHM) and we detect no other stars within the full $10''$ field of view. We estimate our sensitivity by injecting simulated sources with $S/N = 5$ into the final combined images at a range of distances from the central source. The 5σ sensitivities, as a function of radius from the star, are shown in Figure 2. At wider separations, 2MASS J-band imagery shows a possible source $11.''2$ north of HD 106315. Because the source is not

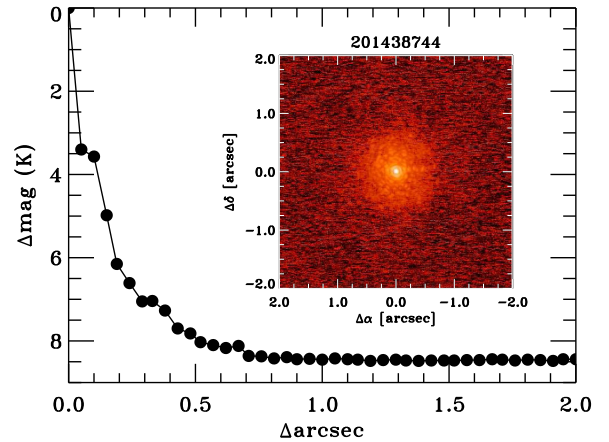


Figure 2. We detect no objects near HD 106315 in archival images or with Keck/NIRC2 adaptive optics, as shown in the image (inset) and the resulting K_s-band contrast curve.

obviously seen in 2MASS H or K, is not in the 2MASS point source catalog, and is not seen in any bands of UKIDSS, Pan-STARRS, or SDSS, we conclude that it is spurious. Therefore, we find no evidence for additional stars within our roughly $40''$ -diameter photometric aperture.

2.3. Planet Validation

Almost all candidates in *Kepler*’s multi-planet systems are *bona fide* planets (Lissauer et al. 2011) rather than non-planetary false positives. Nonetheless, we carry out a full statistical validation of both transit signals orbiting HD 106315. As described above, our HIRES spectrum shows no evidence for secondary spectral lines and our NIRC2 images show no evidence for secondary stellar sources. Furthermore, the stellar density inferred from each planet’s light-curve fit (assuming a circular orbit; $\rho_{*,\text{circ}}$) is consistent with the stellar density from our SpecMatch analysis. All of these lines of evidence are consistent with a planetary interpretation of the observed transits.

Therefore, we follow our previous approach (Crossfield et al. 2016; Schlieder et al. 2016) and use VESPA (Morton 2012) along with the NIRC2 contrast constraints and HIRES secondary line constraints to measure the false positive probability (FPP) of each transit signal, finding $\text{FPP} = 4.3 \times 10^{-4}$ and 5.1×10^{-5} for planets b and c, respectively. Because we see two transit-like signals, each receives a multiplicity boost that further reduces the FPPs (Sinukoff et al. 2016). Thus, we conclude that HD 106315

indeed hosts two transiting planets, whose parameters are summarized in Table 2.

3. Discussion

Our analysis indicates two sub-Jovian planets transiting HD 106315, a bright ($V=8.95$) star, with orbital periods and radii of 9.55 days and 21.1 days, and $2.23^{+0.30}_{-0.25} R_{\oplus}$ and $3.95^{+0.42}_{-0.39} R_{\oplus}$, respectively. An RV trend of $0.3 \pm 0.1 \text{ m s}^{-1} \text{ day}^{-1}$ hints at the presence of a third body at longer orbital periods. The stellar parameters are summarized in Table 1, and the planetary parameters are given in Table 2. Below, we discuss constraints on the masses, orbits, and stability of the objects orbiting HD 106315, and then discuss future prospects for study of this system.

3.1. Orbital Dynamics

Our current RV data are insufficient to measure any planet masses, but numerous planets with measured masses are known in the $2\text{--}4 R_{\oplus}$ size range (Wright et al. 2011). Examination of the current mass–radius diagram allows us to estimate masses of 8 and $20 M_{\oplus}$ for planets b and c, respectively; these estimates are likely good to roughly a factor of two, due to the observed diversity of envelope fractions among sub-Neptunes (Weiss et al. 2016b; Wolfgang et al. 2016). Predictive formulae derived from planetary mass–radius measurements give results consistent with our estimate. With these nominal masses, the planets would induce RA signals with semi-amplitudes of roughly 2.3 and 4.4 m s^{-1} , respectively—not too far below the system’s RV scatter, indicating that mass measurements will be feasible. Indeed, our preliminary RV analysis summarized in Table 4 hints that the signals from planets b and c may be detectable and perhaps larger than predicted in the preceding discussion. Further observations are needed if we are to adequately sample the two planets’ orbits, disentangle the two planets’ signals from other possible RV noise sources, and robustly measure these planets’ masses.

The RV trend we detect indicates that a third body may also orbit HD 106315 at wider separations than planets b and c. As we do not detect any curvature, we sample $\lesssim 25\%$ of this body’s orbit, and its period is $\gtrsim 160$ days. Following Winn et al. (2009), for a circular orbit, the minimum mass and semimajor axis of this third object must satisfy

$$\frac{M_3 \sin i}{a_3^2} \approx (200 \pm 60) M_{\oplus} \text{ AU}^{-2}. \quad (1)$$

Assuming no RV curvature, we know that $a_3 \gtrsim 0.6 \text{ AU}$, and so the third object has $M_3 \sin i \gtrsim 45 M_{\oplus}$. Such an object should be at least the size of Neptune and induce a transit depth of $\gtrsim 0.1\%$, which is easily ruled out by the photometry shown in Figure 1. If the trend-inducing object orbits beyond roughly 4.6 AU , it would have the mass of a brown dwarf, and if orbiting beyond 11.4 AU , it must be a star.

Although the two transiting planets are not closely spaced ($a_c/a_b=1.7$), we also evaluate the system’s stability. The relevant length scale for dynamical interactions between planets is the mutual Hill radius, R_H (Fabrycky et al. 2012). Using the planet masses assumed above, the separation between the two planets is $17.4 R_H$, much greater than the minimum separation of ≈ 3.5 necessary for long-term stability (Gladman 1993). Even if both masses were twice as large, the separation decreases to only $13.8 R_H$. Therefore, we conclude that the two planets transiting HD 106315 do not violate the

criterion of Hill stability; this conclusion is also consistent with the observation that many systems discovered by *Kepler* and RV surveys are even more compact. Indeed, there is still plenty of room: by the above criterion, the system would remain stable even if another $20 M_{\oplus}$ warm Neptune orbited between the two transiting planets. The 21 days planet and the third orbiting body are also Hill stable, having $a_3/a_c > 2.6$ and being separated by $> 13 R_H$.

Although the system is likely to be dynamically stable, mutual gravitational perturbations could still cause measurable transit timing variations (TTVs). Quantifying the amplitude of any TTVs could more tightly constrain the masses and orbits than could the RVs alone (Holman et al. 2010; Nesvorný et al. 2013; Weiss et al. 2016a, 2016b; Sinukoff et al. 2017). Assuming the above planet masses and zero eccentricity, and using the *TTVFaster* code of Agol & Deck (2016), we estimate that TTV amplitudes of up to five minutes could be expected for planet b (whose mass is presumably lower) and less for planet c. These TTV amplitudes would tend to increase if either planet has significant eccentricity, which would be plausible given their small sizes and orbital periods. If HD 106315 c’s period is not strictly regular, the uncertainty in its orbital period could be larger than that reported in Table 2. With the entire C10 data set, we measure HD 106315 b’s time-of-transit with a precision of only 6.5 minutes, so we see no evidence of TTVs in our *K2* data. Nonetheless, precise follow-up transit photometry might detect such TTVs and would also be sensitive to additional planets not observed to transit during *K2*’s C10 observations. We have planned *Spitzer* transit observations of both planets (GO-13052, PI Werner) to search for TTVs and refine the orbital parameters of both transiting planets.

3.2. Follow-up Opportunities

Because it is bright and because all three bodies orbiting it should induce measurable RA signals, HD 106315 will be a useful target. Despite the star’s rapid rotation and its RA scatter of roughly 6.4 m s^{-1} , our existing observations already suggest that frequent RV measurements should be able to measure the transiting planets’ masses and constrain their approximate bulk compositions, and map the orbit and measure the mass of the third orbiting body.

Another interesting avenue is the mostly unexplored spin–orbit alignment of sub-Jovian planets. Though many successful measurements of the Rossiter–McLaughlin (RM) effect and of transit tomography have been made for hot Jupiters, no conclusive RM measurements have been made for sub-Neptune-sized planets (however, see Albrecht et al. 2013; Bourrier & Hébrard 2014; López-Morales et al. 2014; Barnes et al. 2015). Following Gaudi & Winn (2007), the estimated amplitudes of the RM effect for planets b and c (assuming spin–orbit alignment) are as much as 4.2 m s^{-1} and 12.7 m s^{-1} , respectively, depending on their (relatively unconstrained) impact parameter. These amplitudes are not large, but should be measurable. Such measurements are especially intriguing given the likely presence of the third long-period body in the system. Depending on its orbit, long-term interactions with the inner transiting planets could have directly impacted their orbital histories, mutual inclinations, and spin–orbit alignments.

Given the apparent brightness of HD 106315, the transiting planets could be useful targets for atmospheric characterization. The system will be observable at high S/N by all *JWST*

instruments in most resolution modes (except the NIRSPEC low resolution mode, which will saturate; Beichman et al. 2014). Considering their sizes, both planets likely have considerable volatile content (Lopez & Fortney 2014; Marcy et al. 2014; Weiss & Marcy 2014; Dressing et al. 2015; Rogers 2015; Wolfgang & Lopez 2015; Wolfgang et al. 2016). Assuming that these planets have atmospheres dominated by H₂/He, the expected amplitude of spectroscopic signals seen in transit would be up to 40 ppm in a cloud-free atmosphere (and greater if the planets are lower-mass than assumed here). Of those exoplanets studied in some detail, HD 106315 c is most similar in size and irradiation to HAT-P-11b (which is slightly larger and more irradiated). HD 106315 b is not especially similar to any exoplanet with a well-studied atmosphere but is of comparable size to and lies midway in irradiation between HD 97658b and 55 Cnc e. Although transmission spectroscopy suggests that the above planets do not have cloud-free atmospheres with a low mean molecular weight (Fraine et al. 2014; Knutson et al. 2014), we expect some sub-Jovian atmospheres to be amenable to transmission spectroscopy if these planets' atmospheres are as diverse as those of hot Jupiters (Sing et al. 2016). The planets' thermal emission could also be detected with *JWST*/MIRI observations. So making the gross assumption that the planets emit as blackbodies, their secondary eclipses have amplitudes of roughly 20 ppm at 5 μ m and 40–100 ppm at the end of the MIRI bandpass. Observations of thermal emission would have the benefit of being relatively unobstructed by any atmospheric aerosols (e.g., Morley et al. 2015).

Thus, the prospects for future characterization are bright for *K2*'s latest multi-planet system. RV spectrographs will quickly measure the planet masses and determine their spin-orbit alignments, and transit and eclipse spectroscopy will constrain their atmospheric makeup. The RV follow-up will also determine the outer body's mass and orbit, further elucidating the system's architecture. These detailed studies will be possible only because they orbit a bright star—among the brightest host stars of any *K2* systems found to date. The exciting prospects for future measurements of HD 106315 only heighten our anticipation for *TESS*, which we hope will find enough such systems around even brighter stars to keep the field busy for many years to come.

This work made use of the SIMBAD database (operated at CDS, Strasbourg, France) and NASA's Astrophysics Data System Bibliographic Services. This research has made use of the NASA Exoplanet Archive and the Infrared Science Archive, which are operated by the California Institute of Technology, under contract with the National Aeronautics and Space Administration. Portions of this work were performed at the California Institute of Technology under contract with the National Aeronautics and Space Administration. Some of the data presented herein were obtained at the WM Keck Observatory (which is operated as a scientific partnership among Caltech, UC, and NASA). The authors wish to recognize and acknowledge the very significant cultural role and reverence that the summit of Mauna Kea has always had within the indigenous Hawaiian community. We are most fortunate to have the opportunity to conduct observations from this mountain. I.J.M.C. was supported for this work under contract with the Jet Propulsion Laboratory (JPL) funded by NASA through the Sagan Fellowship Program executed by the

NASA Exoplanet Science Institute. A.W.H. acknowledges support for this *K2* work from a NASA Astrophysics Data Analysis Program grant, support from the *K2* Guest Observer Program, and a NASA Key Strategic Mission Support Project. L.M.W. acknowledges support from the Trottier family.

Facility: Kepler, Keck-II (NIRC2), Keck-II (HIRES).

Note added in review. While preparing this paper, we became aware of another paper describing the identification of HD 106315 as a planet-hosing system (Rodriguez et al. 2017). We are pleased that both groups report consistent results despite the fact that no detailed information was shared prior to submission of the two papers.

References

- Agol, E., & Deck, K. 2016, *ApJ*, **818**, 177
- Albrecht, S., Winn, J. N., Marcy, G. W., et al. 2013, *ApJ*, **771**, 11
- Barnes, J. W., Ahlers, J. P., Seubert, S. A., & Relles, H. M. 2015, *ApJL*, **808**, L38
- Beichman, C., Benneke, B., Knutson, H., et al. 2014, *PASP*, **126**, 1134
- Berta-Thompson, Z. K., Irwin, J., Charbonneau, D., et al. 2015, *Natur*, **527**, 204
- Borucki, W. J., Koch, D., Basri, G., et al. 2010, *Sci*, **327**, 977
- Bourrier, V., & Hébrard, G. 2014, *A&A*, **569**, A65
- Ceillier, T., van Saders, J., García, R. A., et al. 2016, *MNRAS*, **456**, 119
- Coughlin, J. L., Mullally, F., Thompson, S. E., et al. 2016, *ApJS*, **224**, 12
- Crossfield, I. J. M. 2015, *PASP*, **127**, 941
- Crossfield, I. J. M., Ciardi, D. R., Petigura, E. A., et al. 2016, *ApJS*, **226**, 7
- Crossfield, I. J. M., Petigura, E., Schlieder, J. E., et al. 2015, *ApJ*, **804**, 10
- Dressing, C. D., & Charbonneau, D. 2013, *ApJ*, **767**, 95
- Dressing, C. D., & Charbonneau, D. 2015, *ApJ*, **807**, 45
- Dressing, C. D., Charbonneau, D., Dumusque, X., et al. 2015, *ApJ*, **800**, 135
- Dumusque, X., Lovis, C., Ségransan, D., et al. 2011a, *A&A*, **535**, A55
- Dumusque, X., Santos, N. C., Udry, S., Lovis, C., & Bonfils, X. 2011b, *A&A*, **527**, A82
- Dumusque, X., Udry, S., Lovis, C., Santos, N. C., & Monteiro, M. J. P. F. G. 2011c, *A&A*, **525**, A140
- Fabrycky, D. C., Ford, E. B., Steffen, J. H., et al. 2012, *ApJ*, **750**, 114
- Figueira, P., Pont, F., Mordasini, C., et al. 2009, *A&A*, **493**, 671
- Foreman-Mackey, D., Hogg, D. W., Lang, D., & Goodman, J. 2012, arXiv:1202.3665
- Fortney, J. J., Mordasini, C., Nettelmann, N., et al. 2013, *ApJ*, **775**, 80
- Fraine, J., Deming, D., Benneke, B., et al. 2014, *Natur*, **513**, 526
- Fressin, F., Torres, G., Charbonneau, D., et al. 2013, *ApJ*, **766**, 81
- Gaia Collab., Brown, A. G. A., Vallenari, A., et al. 2016, *A&A*, **595**, A2
- Galland, F., Lagrange, A.-M., Udry, S., et al. 2005, *A&A*, **443**, 337
- Gaudi, B. S., & Winn, J. N. 2007, *ApJ*, **655**, 550
- Gladman, B. 1993, *Icar*, **106**, 247
- Haywood, R. D., Collier Cameron, A., Queloz, D., et al. 2014, *MNRAS*, **443**, 2517
- Holman, M. J., Fabrycky, D. C., Ragozzine, D., et al. 2010, *Sci*, **330**, 51
- Houk, N., & Swift, C. 1999, in Michigan Spectral Survey, Vol. 5, Michigan Catalogue of Two-dimensional Spectral Types for the HD Stars (Ann Arbor, MI: Dep. Astron., Univ. Michigan), 0
- Howard, A. W., Johnson, J. A., Marcy, G. W., et al. 2010a, *ApJ*, **721**, 1467
- Howard, A. W., Marcy, G. W., Bryson, S. T., et al. 2012, *ApJS*, **201**, 15
- Howard, A. W., Marcy, G. W., Johnson, J. A., et al. 2010b, *Sci*, **330**, 653
- Howell, S. B., Sobek, C., Haas, M., et al. 2014, *PASP*, **126**, 398
- Huber, D., Bryson, S. T., Haas, M. R., et al. 2016, *ApJS*, **224**, 2
- Isaacson, H., & Fischer, D. 2010, *ApJ*, **725**, 875
- Kjeldsen, H., & Bedding, T. R. 1995, *A&A*, **293**, 87
- Knutson, H. A., Dragomir, D., Kreidberg, L., et al. 2014, *ApJ*, **794**, 155
- Kolbl, R., Marcy, G. W., Isaacson, H., & Howard, A. W. 2015, *AJ*, **149**, 18
- Kreidberg, L. 2015, *PASP*, **127**, 1161
- Lissauer, J. J., Fabrycky, D. C., Ford, E. B., et al. 2011, *Natur*, **470**, 53
- Lopez, E. D., & Fortney, J. J. 2014, *ApJ*, **792**, 1
- López-Morales, M., Triaud, A. H. M. J., Rodler, F., et al. 2014, *ApJL*, **792**, L31
- Marcy, G. W., & Butler, R. P. 1992, *PASP*, **104**, 270
- Marcy, G. W., Isaacson, H., Howard, A. W., et al. 2014, *ApJS*, **210**, 20
- Morley, C. V., Fortney, J. J., Marley, M. S., et al. 2015, *ApJ*, **815**, 110
- Morton, T. D. 2012, *ApJ*, **761**, 6
- Moses, J. I., Line, M. R., Visscher, C., et al. 2013, *ApJ*, **777**, 34

- Nesvorný, D., Kipping, D., Terrell, D., et al. 2013, *ApJ*, 777, 3
- Parviainen, H., & Aigrain, S. 2015, *MNRAS*, 453, 3821
- Petigura, E. A. 2015, arXiv:1510.03902
- Petigura, E. A., Howard, A. W., & Marcy, G. W. 2013a, *PNAS*, 110, 19273
- Petigura, E. A., Marcy, G. W., & Howard, A. W. 2013b, *ApJ*, 770, 69
- Ricker, G. R., Winn, J. N., Vanderspek, R., et al. 2014, *Proc. SPIE*, 9143, 20
- Rodríguez, J. E., Zhou, G., Vanderburg, A., et al. 2017, arXiv:1701.03807
- Rogers, L. A. 2015, *ApJ*, 801, 41
- Rogers, L. A., Bodenheimer, P., Lissauer, J. J., & Seager, S. 2011, *ApJ*, 738, 59
- Rogers, L. A., & Seager, S. 2010, *ApJ*, 716, 1208
- Schlieder, J. E., Crossfield, I. J. M., Petigura, E. A., et al. 2016, *ApJ*, 818, 87
- Sing, D. K., Fortney, J. J., Nikolov, N., et al. 2016, *Natur*, 529, 59
- Sinukoff, E., Howard, A. W., Petigura, E. A., et al. 2016, *ApJ*, 827, 78
- Sinukoff, E., Howard, A. W., Petigura, E. A., et al. 2017, *AJ*, 153, 70
- Sullivan, P. W., Winn, J. N., Berta-Thompson, Z. K., et al. 2015, *ApJ*, 809, 77
- Vanderburg, A., Becker, J. C., Kristiansen, M. H., et al. 2016a, *ApJL*, 827, L10
- Vanderburg, A., Bieryla, A., Duev, D. A., et al. 2016b, *ApJL*, 829, L9
- Vanderburg, A., Latham, D. W., Buchhave, L. A., et al. 2016c, *ApJS*, 222, 14
- Vogt, S. S., Allen, S. L., Bigelow, B. C., et al. 1994, *Proc. SPIE*, 2198, 362
- Weiss, L. M., Deck, K., Sinukoff, E., et al. 2016a, arXiv:1612.04856
- Weiss, L. M., & Marcy, G. W. 2014, *ApJL*, 783, L6
- Weiss, L. M., Rogers, L. A., Isaacson, H. T., et al. 2016b, *ApJ*, 819, 83
- Winn, J. N., & Fabrycky, D. C. 2015, *ARA&A*, 53, 409
- Winn, J. N., Johnson, J. A., Fabrycky, D., et al. 2009, *ApJ*, 700, 302
- Wolfgang, A., & Lopez, E. 2015, *ApJ*, 806, 183
- Wolfgang, A., Rogers, L. A., & Ford, E. B. 2016, *ApJ*, 825, 19
- Wright, J. T., Fakhouri, O., Marcy, G. W., et al. 2011, *PASP*, 123, 412